Cell, Vol. 114, 457–467, August 22, 2003, Copyright ©2003 by Cell Press

The *Drosophila* Mst Ortholog, *hippo*, Restricts Growth and Cell Proliferation and Promotes Apoptosis

Kieran F. Harvey,[1] Cathie M. Pfleger,[1] and Iswar K. Hariharan*
Massachusetts General Hospital Cancer Center
Building 149, 13th Street
Charlestown, Massachusetts 02129

Summary

Establishing and maintaining homeostasis is critical to the well-being of an organism and is determined by the balance of cell proliferation and death. Two genes that function together to regulate growth, proliferation, and apoptosis in *Drosophila* are *warts* (*wts*), encoding a serine/threonine kinase, and *salvador* (*sav*), encoding a WW domain containing Wts-interacting protein. However, the mechanisms by which *sav* and *wts* regulate growth and apoptosis are not well understood. Here, we describe mutations in *hippo* (*hpo*), which encodes a protein kinase most related to mammalian Mst1 and Mst2. Like *wts* and *sav*, *hpo* mutations result in increased tissue growth and impaired apoptosis characterized by elevated levels of the cell cycle regulator cyclin E and apoptosis inhibitor DIAP1. Hpo, Sav, and Wts interact physically and functionally, and regulate DIAP1 levels, likely by Hpo-mediated phosphorylation and subsequent degradation. Thus, Hpo links Sav and Wts to a key regulator of apoptosis.

Introduction

Both organism size and cell number are determined by the extent of growth, cell proliferation, and cell death that occur during development. Genetic studies in *Drosophila* have helped define some of the pathways that regulate each of these processes. Many of these studies have examined the development of the imaginal discs, groups of epithelial cells of the larva and pupa that generate many parts of the adult fly, including the eye and wing. Important regulators of growth include the insulin-mediated signaling pathway, Tor, Myc, Ras, cyclin D/cdk4, and the tuberous sclerosis complex (Tsc) proteins (reviewed by Oldham and Hafen, 2003; Marygold and Leevers, 2002). Programmed cell death is regulated by interplay between proapoptotic proteins such as Reaper (Rpr) (White et al., 1994), Hid (Grether et al., 1995), and Grim (Chen et al., 1996) and the inhibitors of apoptosis (e.g., DIAP1) (Goyal et al., 2000; Lisi et al., 2000; Wang et al., 1999). Together, they determine the activity level of cellular caspases. Other molecules that regulate cell death include the p53 protein and the bcl2 family members (reviewed by Richardson and Kumar, 2002).

Two genes that appear to function together to regulate growth, cell proliferation, and cell death in *Drosophila* are *warts* (*wts*) (Justice et al., 1995; Xu et al., 1995) and *salvador* (*sav*) (Kango-Singh et al., 2002; Tapon et al., 2002). Clones of homozygous mutant *wts* or *sav* cells outgrow their wild-type neighbors (Kango-Singh et al., 2002; Tapon et al., 2002). Moreover, the mutant cells are relatively resistant to the developmentally regulated apoptosis that normally eliminates supernumerary cells. *wts* encodes a ser/thr kinase related to the NDR and Dbf2 kinases, while *sav* encodes a protein with motifs implicated in protein-protein interactions, including a WW domain that is capable of interacting with PPXY motifs found in Wts. The phenotypic similarity of *wts* and *sav* mutant cells, as well as the demonstrated ability of Sav to bind to Wts (Tapon et al., 2002), suggest that these two proteins may function together to restrict growth and promote apoptosis. However, the mechanisms by which Wts and Sav regulate growth and cell death are still not well understood.

Here, we present a phenotypic and molecular characterization of the *Drosophila hippo* (*hpo*) gene. Mutations in *hpo* elicit phenotypes that are similar to those observed in *sav* or *wts*. *hpo* encodes a serine-threonine protein kinase of the STE20 family and is most related to the mammalian Mst2 (or krs1) kinase. Our experiments link the Sav/Wts pathway to known regulators of apoptosis via Hpo.

Results

We have screened for genes that restrict growth and cell number by generating clones of homozygous mutant cells and sister clones of wild-type cells in the eyes of otherwise heterozygous animals. Mutant and wild-type tissue are identified by the presence of eye color markers (mutant tissue is white; wild-type tissue is red) and thus their relative contribution to the adult eye can be assessed. We retain flies that have an overrepresentation of mutant as compared to wild-type tissue. Mutations identified thus far include multiple alleles of the Tuberous sclerosis complex genes (*Tsc1* and *Tsc2*), *archipelago* (*ago*), *sav*, and *wts*. Here, we describe from our screen of the right arm of chromosome 2, *hpo,* a gene that regulates cell growth, cell cycle exit, and cell death.

hpo Regulates Cell Number and Organ Size

We identified three alleles of a gene that we termed *hippo* (*hpo*). All three alleles are lethal either when homozygous or in trans to another allele. Eyes containing *hpo* mutant clones (white tissue) and wild-type clones (red tissue) have an overrepresentation of mutant tissue (Figure 1B) when compared to eyes containing clones of the wild-type parental FRT42D chromosome (Figure 1A) suggesting that the mutant tissue may have a relative growth advantage. A close-up of an eye mosaic for *hpo* shows that mutant ommatidial facets are slightly larger than wild-type facets and sometimes contain extra interommatidial bristles (Figure 1C). When homozygous clones of *hpo* were generated in other imaginal discs using *hsFLP*, outgrowths of tissue were observed (data

*Correspondence: hariharan@helix.mgh.harvard.edu
[1]These authors contributed equally to this work.

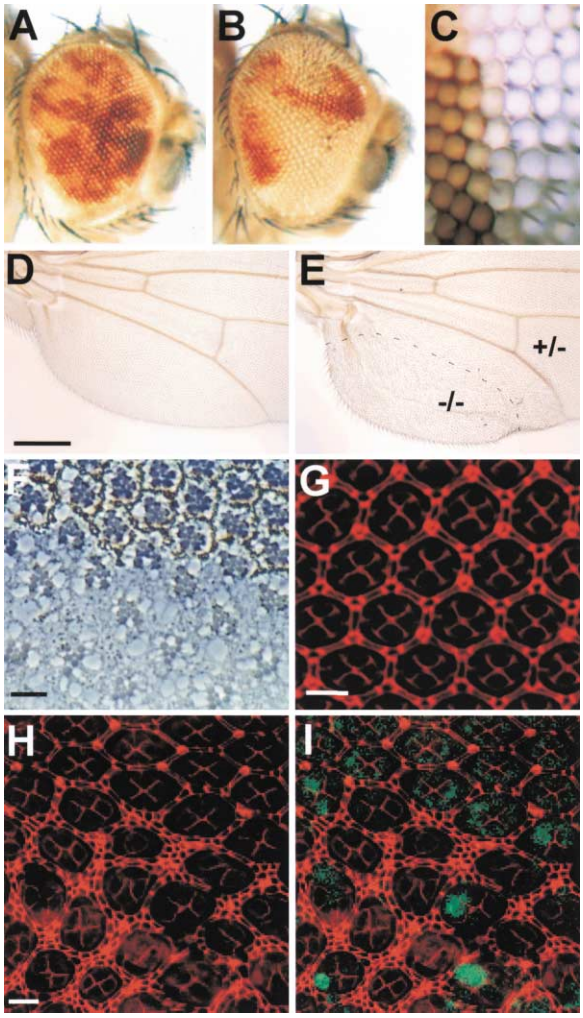

Figure 1. Mutations in *hpo* Lead to Increased Cell Growth and Number

(A and B) Adult eyes containing clones of red tissue (wild-type) and white tissue (parent chromosome in A, *hpo* in B). *hpo* mosaic eyes have an overrepresentation of mutant tissue compared to the parent chromosome.

(C) Close-up of an adult eye mosaic for wild-type tissue (red) and *hpo* tissue (white). *hpo* ommatidial facets appear larger than wild-type and have extra bristles.

(D and E) Wild-type adult wing (D) and a wing mostly heterozygous for *hpo* (+/−) that contains a large *hpo* clone (−/−) indicated by a dashed line (E). The wing compartment containing the *hpo* mutant clone is enlarged.

(F) Retinal section of an adult eye mosaic for *hpo* (mutant tissue lacks pigment). Extra tissue is observed between the rhabdomere clusters of adjacent ommatidia.

(G–I) Cell outlines in 48 hr pupal eye discs visualized by staining with anti-Discs-large antibody.

(G) Wild-type discs possess a single layer of interommatidial cells.

(H and I) *hpo* mosaic eye disc showing additional interommatidial cells in mutant clones compared to wild-type (GFP positive, green). Scale bar is equal to 200 μM for (D) and (E), 20 μM for (F), and 10 μM for (G–I).

not shown) and portions of wings containing large *hpo* clones (Figure 1E) were larger than the corresponding portion of a wild-type wing (Figure 1D), indicating a role for *hpo* in regulating organ size in tissues other than the eye. Retinal sections of adult eyes containing *hpo* clones revealed that mutant ommatidia appear to have the normal complement and arrangement of photoreceptor cells (Figure 1F). However, *hpo* mutant ommatidia appeared to have significantly more tissue between adjacent ommatidia. Cell outlines are visualized more readily in the pupal retina (Figures 1G–1I). In contrast to the single layer of interommatidial cells observed in wild-type retinas, mutant ommatidia have several additional interommatidial cells (Figures 1G–1I). These phenotypic abnormalities are very similar to those observed in *sav* or *wts* mutant clones (Kango-Singh et al., 2002; Tapon et al., 2002).

hpo Is Required for Cell Cycle Exit and Regulates Expression of *cyclin E*

sav or *wts* mutant cells in the eye imaginal disc fail to exit from the cell cycle at the appropriate time. The additional rounds of cell division generate an excess of interommatidial cells. Elevated levels of cyclin E protein detected in mutant cells may underlie the delayed cell cycle exit (Kango-Singh et al., 2002; Tapon et al., 2002).

In a disc mosaic for the wild-type parent chromosome, BrdU-incorporation was evident in the anterior portion of the disc and in a narrow stripe, the second mitotic wave (SMW), but not in the morphogenetic furrow (MF) or posterior to the SMW where cells arrest in the G1 phase of the cell cycle (Figure 2A). In *hpo* mosaic eye discs, the pattern of S phases was normal in the anterior portion of the disc and in the SMW but in mutant portions of the disc, BrdU-incorporating nuclei were observed posterior to the SMW and also in the MF (Figure 2B). Thus, *hpo* cells continue to cycle when surrounding wild-type cells (GFP-positive) are arrested in G1, indicating that *hpo* function is essential for timely cell cycle exit. In discs containing clones of the wild-type parental chromosome, mitoses, visualized with anti-phospho histone H3, were observed in the anterior portion of the eye disc and in several rows of developing ommatidia immediately posterior to the SMW (Figure 2C). In discs mosaic for *hpo* however, extra mitoses were seen in mutant clones many ommatidial rows posterior to the SMW (Figure 2D) indicating that at least a subset of *hpo* mutant cells continue to divide when wild-type cells are mitotically quiescent. These abnormalities are similar to, though less severe than, those found in *sav* and *wts* imaginal discs (Kango-Singh et al., 2002; Tapon et al., 2002).

Elevated levels of cyclin E were found in *hpo* mutant clones immediately anterior to the MF, in the SMW, and posterior to the SMW (Figures 2E–2H). Cyclin E expression appeared normal in *hpo* clones in the most anterior portions of the third instar larval eye-antennal disc. In contrast, cyclins A, B, and D were expressed at normal levels throughout the disc (data not shown). In wild-type discs *cyclin E* RNA is expressed in a narrow stripe corresponding to the SMW. In discs mosaic for *hpo*, the level of *cyclin E* RNA was elevated and the expression domain of *cyclin E* was broader (data not shown). Additionally, an increase in *cyclin E* mRNA was detected by semiquantitative RT-PCR performed on eye imaginal discs composed almost entirely of *hpo* mutant tissue (Supplemental Figure S1C available at http://

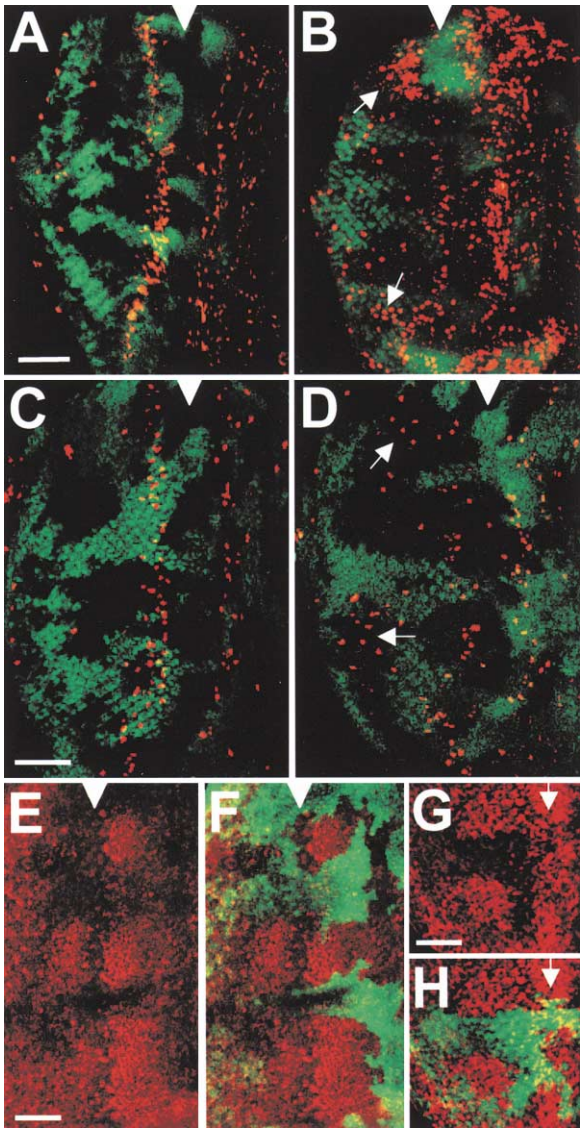

Figure 2. *hpo* Mutations Cause a Delay in Cell Cycle Exit, Likely Due to Increased Levels of Cyclin E

Third instar larval eye discs, anterior is to the right.

(A–D) Tissue homozygous for either the parent FRT42D chromosome (A and C) or the *hpo* chromosome (B and D) fails to express GFP (green). The MF is marked by arrowheads.

(A and B) S phases visualized by BrdU-incorporation (red) in discs mosaic for the parent chromosome (A) or *hpo* (B). BrdU-incorporation posterior to the SMW is evident in *hpo* mutant clones (indicated by arrows in B) but only as a single stripe corresponding to the SMW in the posterior portion of wild-type discs (A).

(C and D) Mitoses evidenced by staining with anti-phospho histone H3 antibody in discs containing clones of tissue derived from the parent chromosome (C) or *hpo* (D). Ectopic mitoses are evident posterior to the SMW in *hpo* mutant tissue (arrows in D). In general, discs containing *hpo* clones are convoluted when compared to wild-type discs and hence not all BrdU incorporation or anti-phospho histone H3 staining is captured in a single confocal section

(E–H) Cyclin E protein staining (red) in discs mosaic for *hpo* as visualized by staining with anti-cyclin E antibody. Elevated levels of cyclin E are seen in mutant clones immediately anterior and posterior to the MF. *hpo* mutant tissue is marked by absence of GFP (green) in (F) and (H). Arrowheads indicate the MF, arrows indicate the SMW. Scale bar is equal to 50 μM for (A–F), 25 μM for (G) and (H).

www.cell.com/cgi/content/full/114/4/457/DC1). This indicates that, at least in part, *hpo* regulates *cyclin E* at the level of transcription or RNA stability but additional posttranscriptional regulation is also possible. In experiments where we reduced *hpo* function in S2 cells by RNAi, the levels of cyclin E protein were increased without an obvious change in RNA levels as assessed by Northern blotting (Supplemental Figures S1D and S1E available on website). Thus, *hpo* may be capable of regulating cyclin E levels at both transcriptional and posttranscriptional levels.

hpo Mutant Cells Are Overrepresented but Have Normal Cell Cycle Phasing and Size

The cycling properties of *hpo* mutant cells were analyzed by generating clones of mutant cells in third instar larval wing discs. Larvae were heat shocked 48 hr after egg deposition (AED) and wing discs were dissected 120 hr AED. Following dissociation with trypsin and staining with Hoechst, cells were subjected to flow cytometry. Cell size, as gauged by forward scatter, and DNA content were measured and found to be almost indistinguishable between wild-type and *hpo* mutant cells (Figures 3A and 3B).

To estimate the doubling time of *hpo* mutant cells with respect to cells derived from the wild-type parental FRT42D chromosome, we counted the cell number in pairs of clones and their wild-type twin spots. Clones were generated at 48 hr AED and analyzed 72 hr later. The number of cells in *hpo* mutant clones was consistently larger than in wild-type sister clones (Figure 3C). The median population doubling time in *hpo* clones was 13.1 hr, which was significantly shorter than that of the GFP-bearing tester chromosome, which was 14.7 hr ($P < 0.0001$ by a Student's paired t test) (Figure 3C). By comparison, clones derived from the parent FRT42D chromosome had a population doubling time that was not significantly different from the same tester chromosome (Figure 3D). It is unlikely that the increased cell numbers in *hpo* clones can be explained by a block in apoptosis, since overexpression of the caspase inhibitor p35 in wing disc cells at this stage of development does not appreciably alter the population doubling time (Prober and Edgar, 2000). Thus, cells appear to divide faster in *hpo* clones. Since cell size is essentially unchanged, this would imply that *hpo* cells have an increased rate of growth (mass accumulation) and a commensurate increase in the rate of cell division.

hpo Is Required for Developmental Cell Death

In wild-type pupal retinas, excess interommatidial cells are eliminated in a wave of apoptosis during the midpupal stage. We have previously shown that there is a defect in apoptosis in *sav* and *wts* mutant tissue (Tapon et al., 2002). As a result, the additional cells generated by excess cell division in *sav* and *wts* tissue are not eliminated and account for the increased number of interommatidial cells.

At a stage of development (38 hr APF) when excess interommatidial cells are eliminated by apoptosis, most of the cell death in discs containing *hpo* clones was restricted to wild-type portions of the disc (Figures 4A–4C). The DIAP1 protein, an antagonist of caspases, is

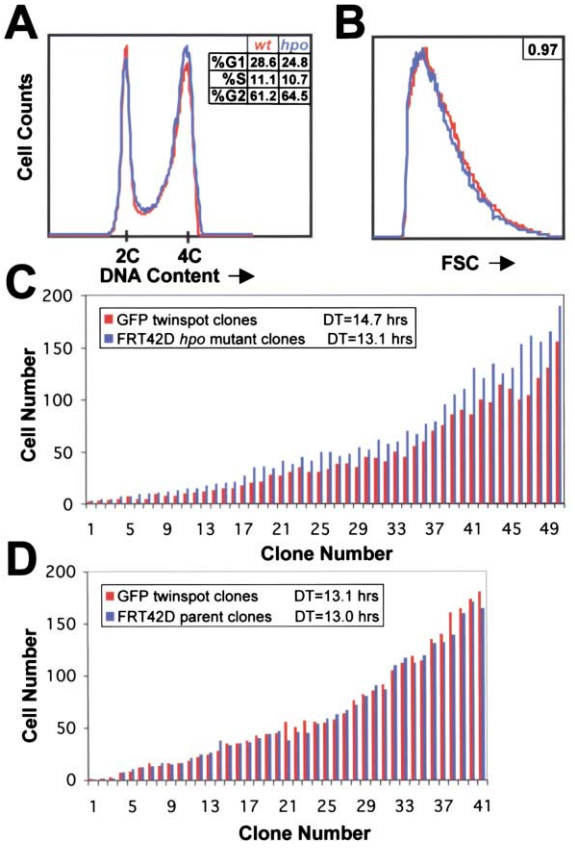

Figure 3. *hpo* Mutant Tissue Has a Growth Advantage

(A and B) DNA content and forward scatter were measured in *hpo* (blue) and wild-type (red) cells from third instar larval wing discs.

(A) DNA content. The percentage of cells inferred to be in each phase of the cell cycle is shown in the inset. (B) Forward scatter. The mean forward scatter of mutant cells as compared to wild-type cells is shown in the inset.

(C and D) Cell number in clone and twinspot pairs plotted in order of increasing cell number. Clones were induced in third instar larval wing discs 48 hr AED and fixed and counted 120 hr AED.

(C) There are more cells in *hpo* clones than in their wild-type sister clones. The calculated population doubling time is 13.1 hr for *hpo* clones compared to 14.7 hr for wild-type GFP twinspot clones.

(D) The number of cells found in wild-type FRT42D parent chromosome clones is almost indistinguishable from the number of cells in GFP twinspot clones.

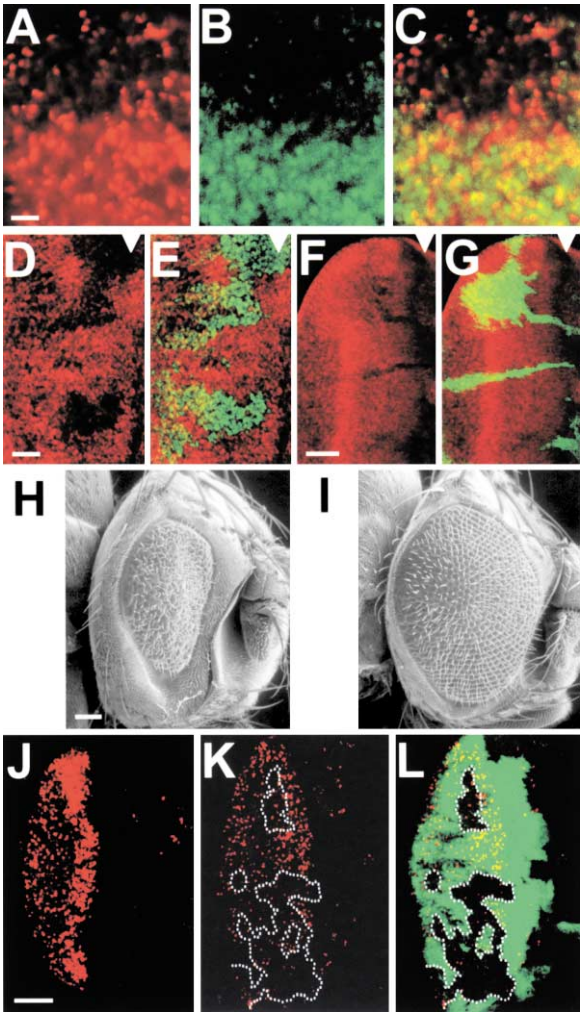

Figure 4. *hpo* is Required for Normal Developmental Cell Death and Grim-Induced Cell Death

(A–C) Developmental cell death in 38 hr pupal eye discs. Cell death in 38 hr pupal eye discs assayed by TUNEL (red in A) is mostly confined to wild-type tissue (green in B) as seen in the merged image (C).

(D–G) Eye discs from third instar larvae, anterior is to the right, and arrowheads indicate the MF. Levels of DIAP1 protein are elevated in *hpo* mutant clones (D and E), and in *wts* mutant clones (F and G). Mutant clones fail to express GFP (E and G).

(H and I) Scanning electron micrographs of adult eyes.

(H) Eyes expressing *GMR-grim* are small and rough.

(I) The small eye size induced by overexpression of *grim* is suppressed by generation of clones of *hpo* mutant tissue.

(J) Cell death measured by TUNEL (red) is evident posterior to the MF in discs expressing *grim* under the control of the GMR promoter.

(K and L) Discs expressing *grim* that contain *hpo* mutant clones (absence of GFP, green in L) have reduced levels of cell death in mutant clones (clonal borders shown by dashed line). Scale bar is equal to 25 μM for (A–C), 50 μM for (D–G) and (J–L), 100 μM for (H) and (I).

elevated in *sav* clones. *hpo* clones posterior to the MF also have elevated DIAP1 levels (Figures 4D and 4E). Regulation of DIAP1 by *hpo* is likely to occur largely at the posttranscriptional level since DIAP1 RNA expression, as assessed by either in situ hybridization or by RT-PCR, was not obviously elevated in eyes composed almost entirely of *hpo* mutant tissue (Supplemental Figures S1A–S1C available on website). DIAP1 RNA expression was also examined in S2 cells treated with RNAi designed to reduce expression of Hpo. Whilst DIAP1 protein levels were increased 1.5-fold in cells treated with Hpo RNAi, no obvious difference in DIAP1 RNA expression was seen (Supplemental Figures S1D and S1E available on website). DIAP1 levels were also elevated in *wts* cells (Figures 4F and 4G). Therefore the defect in apoptosis in *sav, wts*, and *hpo* tissue is likely due to the result of elevated levels of DIAP1 in mutant clones that renders caspases inactive in these cells.

Proteins such as Hid, Rpr, and Grim are thought to downregulate DIAP1 levels by stimulating its autoubiquitination or by repressing general protein translation, which has the greatest effect on short-lived proteins

such as DIAP1 (Hays et al., 2002; Holley et al., 2002; Ryoo et al., 2002; Wilson et al., 2002; Wing et al., 2002; Yoo et al., 2002). To investigate whether *hpo* can modify the function of such proteins, *hpo* clones were generated in flies overexpressing the *grim* gene (Chen et al., 1996) under the control of the GMR promoter. When overexpressed in the *Drosophila* eye, *grim* induces extensive cell death as visualized by TUNEL (Figure 4J), which results in a small, rough eye (Figure 4H). When *hpo* clones were generated in eyes overexpressing Grim, eye size was significantly restored (Figure 4I) and Grim-induced cell death was greatly reduced in *hpo* mutant clones (Figures 4K and 4L). We have previously shown that *sav* and *wts* clones are relatively resistant to cell death induced by Rpr or Hid (Tapon et al., 2002). The increased basal level of DIAP1 found in *sav*, *wts*, or *hpo* clones may make it more difficult for proteins such as Rpr, Hid, or Grim to reduce DIAP1 levels sufficiently to activate caspases in these cells.

Molecular Characterization of the *hpo* Locus

Using recombination mapping (see Experimental Procedures), the *hpo* locus was narrowed to a 165 kb interval between 56D2 and 56D15-56E1 that includes 29 annotated ORFs. The CG11228 gene, found in this interval, has been annotated as the *Drosophila* ortholog of Mst2, a kinase that has been shown to induce apoptosis in mammalian cells. We therefore sequenced this ORF from each of the three *hpo* chromosomes and in each case found single point mutations that generate premature stop codons (Figures 5A and 5D).

CG11228 encodes a protein predicted to be a serine/threonine kinase of the Sterile 20 (STE20) group and most resembles the human Mst2 (also known as Krs1) and Mst1 (also known as Krs2) genes (Figures 5A and 5D) (Creasy and Chernoff, 1995a, 1995b; Taylor et al., 1996). While *hpo* is most similar to Mst2, BLAST searches of the fly genome do not reveal a second Mst1-like gene, suggesting that *hpo* may represent both Mst genes in *Drosophila*. Hpo has an N-terminal kinase domain that is highly conserved between *Drosophila* and human, as well as a conserved C-terminal region that includes a dimerization domain and a potential nuclear localization signal. Human Mst proteins have been reported to be cleaved by caspases during apoptosis (Lee et al., 1998). A potential caspase cleavage site exists in Hpo, although the regions surrounding this site do not share much sequence similarity with human Mst1 and Mst2.

Each of the *hpo* alleles has a C to T base change, which alters the CAG coding for a glutamine to a TAG stop codon at positions 504 (hpo^{MGH1}), 315 (hpo^{MGH2}), and 621(hpo^{MGH3}). While the amino acid sequence reported for Hpo from the strain utilized in the genome project predicts a polyglutamine stretch of 14 residues (residues 490 to 503), the wild-type parental FRT42D strain used in our mutagenesis screen possesses a stretch of 17 glutamines. To avoid confusion, we have maintained the numbering system used by the genome project for the residues C-terminal to the polyglutamine stretch. The hpo^{MGH1} mutation occurs in the 15th glutamine of this stretch, corresponding to Q504 for the FRT42D chromosome. hpo^{MGH2} is predicted to generate the shortest polypeptide ending just C-terminal to the kinase domain, and the longest protein, encoded by hpo^{MGH3}, lacks most of the conserved C-terminal region predicted to include the nuclear localization signal and dimerization domain. Since all three alleles leave the kinase domain intact, it is conceivable that none represents a true null allele and may not abolish all functions of *hpo*. Nevertheless, all three alleles are lethal in trans to each other and eyes containing clones of each of the three *hpo* alleles have a comparable phenotype. Moreover, *hpo* RNAi-treated S2 tissue culture cells also have elevated levels of cyclin E and DIAP1 protein expression (Supplemental Figure S1E available on website). Thus, the alleles identified in our screen likely result in a reduction in *hpo* activity.

Human Mst kinases were originally characterized as proteins that were activated in response to cellular stresses (Taylor et al., 1996). Hpo and Mst kinases belong to a large family of proteins that have a kinase domain similar to that of the yeast Sterile 20 protein, which is thought to be a mitogen-activated protein kinase kinase kinase kinase (Map4K) (Dan et al., 2001). MAP4Ks possess a conserved kinase domain and are postulated to function at the apical point in Map kinase signaling cascades, which have been reported to regulate diverse biological functions including cellular growth, proliferation, differentiation, and apoptosis (Chang and Karin, 2001). Hpo may trigger activation of one or more MAPK pathways and indeed Mst1 and/or Mst2 have been shown to activate Jun N-terminal kinase (JNK) in mammalian cells (Graves et al., 1998). Recently human Mst1 has been shown to directly phosphorylate histone H2B and may mark chromatin for condensation during apoptosis (Cheung et al., 2003). Mst can also bind via its C terminus to a family of proteins lacking known enzymatic domains that include NORE and can function in a proapoptotic pathway downstream of Ki-Ras in mammalian cells (Khokhlatchev et al., 2002).

Imaginal discs from third-instar larvae were probed with either an antisense *hpo* probe (Figure 5B) or a control sense *hpo* probe (Figure 5C). *hpo* was expressed in an unpatterned fashion throughout all imaginal discs including the eye imaginal disc (Figure 5B).

hpo Interacts with *sav* and *wts*

The similarity of the *wts*, *sav*, and *hpo* mutant phenotypes suggests that the three genes function in the same pathway and that all three proteins may exist in the same protein complex. The Sav protein has domains capable of interacting with other proteins, including a WW domain and a C-terminal portion that is predicted to form a coiled-coil. Sav may therefore function as a scaffold in a multiprotein complex. We have previously shown that the WW domains of Sav can bind to the PPXY motifs in the N-terminal portion of Wts (Tapon et al., 2002). We tested whether Hpo could also bind to Sav. Sav was expressed in *E. coli* as a fusion with maltose binding protein (MBP). After stringent washing, MBP-tagged Sav (MBP-Sav) coupled to amylose resin showed significant binding to in vitro translated (IVT) Hpo but MBP coupled to amylose resin did not (Figure 6A). Hpo also bound to IVT Sav expressed as a Myc-tagged fusion (MTSav), but not to the MT alone (Figure 6B). Parallel binding experiments with proteins corre-

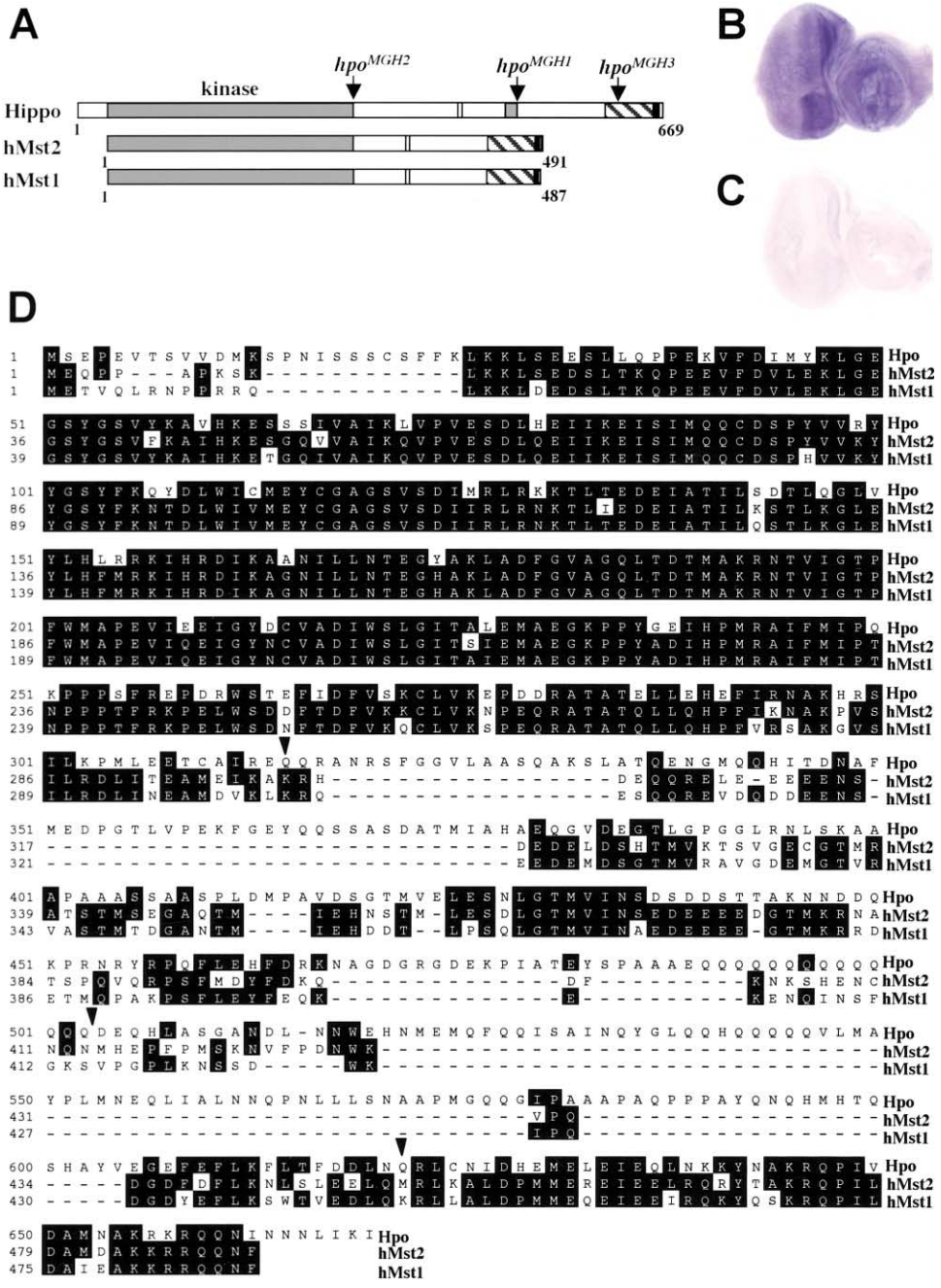

Figure 5. *hpo* Encodes a Protein Kinase that Is Most Similar to Human Mst1 and Mst2

(A) Schematic representation of *Drosophila* Hippo and its two human orthologs, hMST2 and hMST1. The N-terminal kinase domain (large gray box) is highly conserved between *Drosophila* and human, as is the C terminus (striped box), which contains a putative nuclear localization signal (black box). Hpo contains a polyglutamine stretch (small gray box) and in a less-conserved region, both *Drosophila* and human proteins contain potential caspase cleavage sites (open box). The mutations found in the three *hpo* alleles described here are indicated with arrows.
(B and C) Eye imaginal discs from third-instar larvae were probed with either an antisense *hpo* probe (B) or a control sense *hpo* probe (C).
(D) *Drosophila* Hpo and its two human orthologs, hMST2 and hMST1 were aligned using the Clustal algorithm of MEGALIGN. The position of the three *hpo* mutations are indicated by arrowheads.

sponding to the truncated versions of Hpo generated by the hpo^{MGH1}, hpo^{MGH2}, and hpo^{MGH3} alleles showed that all three mutant proteins had markedly reduced in vitro binding to both MT-Sav (Figure 6B) and MBP-Sav (data not shown). These experiments indicate that the C-terminal portion of Hpo is necessary for binding to Sav. Since the protein encoded by the hpo^{MGH3} allele lacks only the C-terminal 49 amino acids, it is likely that Sav interacts with the conserved C-terminal domain of Hpo. Alternatively, conformational changes induced by the deletion of the C-terminal portion may preclude interaction with Sav.

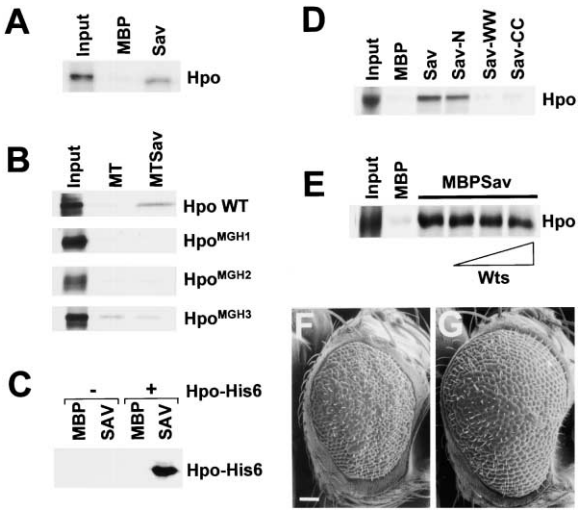

Figure 6. Hpo Interacts Physically with Sav and Is Required for *sav* and *wts*-Induced Apoptosis

(A) IVT Hpo was incubated with either MBP or MBPSav coupled to amylose resin. 10% input of IVT Hpo is shown in the left lane.

(B) Wild-type and mutant Hpo proteins were incubated with either an IVT Myc-tag (MT) or IVT MTSav (MTSav). Hpo mutant proteins corresponding to those generated by the three mutant alleles identified in our screen did not show increased binding to MTSav when compared to interaction with the MT control.

(C) Sav fused to MBP or MBP alone were incubated with partially purified His-tagged Hpo (+) or control bacterial lysate (−), and immunoblotted with anti-His antibody.

(D) Binding of wild-type IVT Hpo to either MBP or portions of Sav fused to MBP (full-length = Sav, the portion N-terminal to the WW domains = Sav-N, WW domains = Sav-WW, and coiled coil region = Sav-CC).

(E) IVT Hpo was incubated with MBPSav (as in A, above) in the presence of increasing amounts of cold IVT Wts.

(F and G) Scanning electron micrographs of adult eyes.

(F) Eyes expressing *sav* and *wts* under the control of the GMR promoter are small and rough.

(G) The small eye size induced by overexpression of *sav* and *wts* is suppressed by generation of clones of *hpo* mutant tissue. Scale bar is equal to 100 μM.

To determine if Sav and Hpo interact directly or via an accessory protein found in reticulocyte lysates, MBP-Sav coupled to amylose resin was incubated with either partially purified bacterial His-tagged Hpo or a control bacterial lysate (Figure 6C). Immunoblotting with an anti-His antibody showed that Hpo interacted with MBP-Sav but not to MBP alone, suggesting that Hpo and Sav can interact with each other directly.

To define the portion of Sav that is capable of interaction with Hpo, we expressed different domains of the Sav protein as fusions with MBP. These fusion proteins were tested for their ability to bind IVT Hpo. Binding of the portion of Sav N-terminal to the WW domain (Sav-N) was comparable to that of full-length Sav (Sav), however no binding was detected with the fusion proteins containing the WW domains of Sav (Sav-WW) or the C-terminal coiled-coil domain (Sav-CC) (Figure 6D). Thus, Hpo appears to bind predominantly to the N-terminal portion of Sav. In further experiments using IVT MTSav domains, some binding of full-length Hpo to the coiled-coil region of Sav was observed (data not shown). This might imply a second site of interaction between the two proteins or be the result of the "stickiness" of the coiled-coil domain.

To examine whether Hpo and Wts bind competitively to Sav or at distinct sites, we tested whether the addition of Wts could reduce the binding of Hpo to Sav by adding increasing amounts of IVT Wts to the binding reaction. Even the addition of four times the amount of Wts as Hpo had no effect on the binding of Hpo to Sav (Figure 6E). This is consistent with the notion that Hpo and Wts bind to different portions of Sav, i.e., the N-terminal portion and the WW domains respectively and is consistent with the possibility that the three proteins can form a ternary complex.

We also examined the interaction of *hpo* with *sav* and *wts* in vivo. Combined overexpression of *sav* and *wts* in the eye generates a small rough eye phenotype, which is mostly due to increased cell death (Tapon et al., 2002). When *hpo* clones were generated in eyes overexpressing both *sav* and *wts*, eye size was significantly restored (Figures 6F and 6G). This suggests that *hpo* is required for the ability of *sav* and *wts* to induce cell death. If, as the binding data suggest, Hpo functions in a complex with Sav and Wts, then Hpo function appears necessary for the proapoptotic activity of the complex.

Regulation of DIAP1 Levels by Hpo

When expressed in cultured cells, the Mst kinases are capable of activating Jun N-terminal kinase (JNK) (Graves et al., 1998). The *basket* gene (*bsk*) encodes the *Drosophila* ortholog of JNK (Riesgo-Escovar et al., 1996; Sluss et al., 1996). DIAP1 levels were normal in *bsk* clones (Figures 7A and 7B) and *bsk* clones did not possess many extra interommatidial cells (Figure 7C). Together these findings suggest that the JNK pathway is not required for *hpo* to regulate DIAP1 and apoptosis. Moreover, *hpo* clones do not modify the extent of cell death induced by overexpression of the TNFα ortholog *eiger* (Igaki et al., 2002; Moreno et al., 2002), which promotes apoptosis in a JNK-dependent pathway (data not shown).

Since DIAP1 protein levels were shown to be elevated in *hpo* clones and in S2 cells treated with *hpo* RNAi, we examined the possibility that *hpo* might regulate DIAP1 stability. When *hpo* was overexpressed in *Drosophila* S2 cells, endogenous DIAP1 protein was consistently reduced to approximately 60–70% of normal levels, when normalized to loading controls (Figure 7D). Since Wts and Hpo are both predicted to have kinase activity, it is possible that a complex consisting of Sav, Hpo, and Wts regulates the phosphorylation state of DIAP1 and hence regulates its turnover. To examine this possibility, we first tested whether proteins that can associate with Sav displayed kinase activity in vitro.

Preliminary experiments using IVT Hpo and IVT control (IVT not supplemented with plasmid encoding *hpo*) demonstrated substantial kinase activity already present in the IVT control. To reduce this background kinase activity, Sav interacting proteins were first purified from IVT and then assayed for their kinase activity. After preincubating bacterially expressed MBP-Sav with either an IVT control or IVT Hpo, we added [γ-^{32}P]ATP in kinase buffer to determine if the MBP-Sav complexes possessed ki-

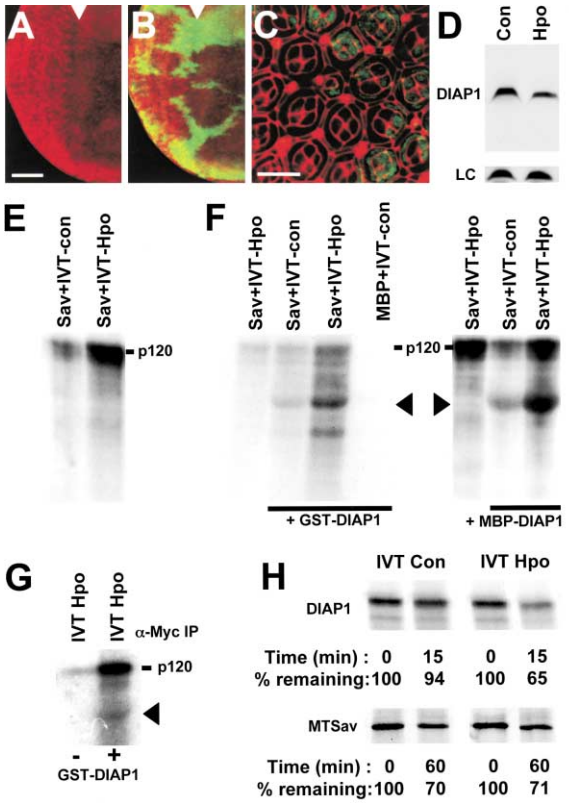

Figure 7. Regulation of DIAP1 Levels by Hpo

(A–B) Third instar larval eye discs, anterior is to the right. *bsk* mutant tissue fails to express β-galactosidase (green). The MF is marked by an arrowhead.

(A and B) The level of DIAP1 protein expression (red) is unchanged between *bsk* mutant and wild-type clones. Scale bar is equal to 50 μM.

(C) Cell outlines in a 48 hr pupal retinal disc containing *bsk* clones (absence of β-galactosidase, green) visualized by staining with anti-Discs-large antibody (red). Scale bar is equal to 20 μM.

(D) Levels of DIAP1 protein in S2 cells transiently transfected with either with an *Actin-Gal4* plasmid (Con) or with both *Actin-Gal4* and *UAS-hpo* plasmids (Hpo) were analyzed using an anti-DIAP1 antibody. Hpo-transfected cells have reduced levels of DIAP1 when compared to control cells and a loading control (LC).

(E) MBP-Sav coupled to amylose resin was incubated with IVT Hpo or IVT control and then incubated with [γ-^{32}P]ATP and kinase buffer. In each case, a phosphorylated 120 kD band (p120) was observed that increased in intensity in lysates containing IVT Hpo.

(F) Either MBP or MBPSav coupled to amylose beads were incubated with an IVT control mix or a IVT Hpo mix. Beads were recovered and incubated with [γ-^{32}P]ATP in the presence or absence of GST-DIAP1 or MBP-DIAP1. As in (E), phosphorylated p120 was observed in the presence of MBPSav but not MBP alone. Modest phosphorylation of DIAP1 was seen in the presence of MBPSav complexes, which increased in the presence of Hpo.

(G) A complex immunopurified from IVT containing MT-Hpo that was incubated with [γ-^{32}P]ATP was capable of phosphorylating p120 as well as GST-DIAP1.

(H) The stability of IVT DIAP1 and IVT MTSav were assayed in the presence of components of the ubiquitin system and either IVT control or IVT Hpo. The amount of DIAP1 and Sav that was present at the indicated time points was calculated using NIH Image. While the rate of degradation of DIAP1 is accelerated by Hpo addition, that of MTSav is not.

nase activity. We consistently observed phosphorylation of a protein with a M_r of approximately 120 kD, which we shall refer to as p120. p120 associated with MBP-Sav from both IVT control and IVT Hpo, and phosphorylation of p120 increased in Hpo-supplemented lysates (Figure 7E). It is conceivable that the Sav-associated kinase activity in control lysates may be due to Mst kinases present in the lysate and that this activity increases when exogenous Hpo is added.

In similar experiments, we found that GST-DIAP1 and MBP-DIAP1 were phosphorylated at a low level by Sav-associated protein complexes, purified from IVT control (Figure 7F). The phosphorylation of either GST-DIAP1 or MBP-DIAP1 and of p120 was increased in the presence of IVT Hpo. When the same experiment was performed using GST or MBP alone as substrates, no phosphorylation was seen (data not shown). Additionally, no phosphorylation of GST-DIAP1 (Figure 7F) or MBP-DIAP1 (data not shown) was observed when incubated with MBP alone and IVT control. Mass spectrometry analysis of phosphorylated GST-DIAP1 identified both a major and minor site of phosphorylation, the former on a peptide with one phosphate added to either Ser 159 or Ser 164 (the analysis could not identify which serine was phosphorylated) and the latter on a peptide with one phosphate added to either Thr 114 or Thr 115 (the analysis could not distinguish between these threonines).

Similarly, we tested whether an Hpo-associated complex could phosphorylate GST-DIAP1 (Figure 7G). Myc-tagged Hpo was immunoprecipitated from the IVT reaction and tested for its ability to phosphorylate GST-DIAP1. Phosphorylation of a protein that comigrates with GST-DIAP1 was observed. Parallel experiments using GST alone as a substrate showed no phosphorylation of GST by the immunoprecipitated Myc-tagged Hpo complex (data not shown). Phosphorylation of GST-DIAP1 was not seen in control experiments, using immunopurified IVT Myc tag alone (data not shown). Thus, both Sav-associated and Hpo-associated complexes are capable of phosphorylating DIAP1 in vitro.

The stability of DIAP1 protein can be regulated by autoubiquitination (Yang et al., 2000; Yoo et al., 2002). One consequence of DIAP1 phosphorylation could be an enhancement of its autoubiquitination. We therefore examined whether DIAP1 stability in reticulocyte lysates supplemented with components of the ubiquitin pathway and an energy-regenerating system was changed by the addition of Hpo. In four independent experiments, DIAP1 protein levels were reduced upon the addition of Hpo, when compared to a control reaction (Figure 7H). In contrast, Hpo did not affect the stability of several control proteins, including Sav (Figure 7H), human cdc2, Drice, Tsc1, and GST (data not shown), even at much later time points. These experiments show that, at least under these conditions, DIAP1 is destabilized in the presence of Hpo, presumably as a result of Hpo-dependent phosphorylation of DIAP1.

Discussion

Hpo Functions Together with Sav and Wts

The phenotypic abnormalities elicited by reducing the activity of either Hpo, Wts, or Sav are extremely similar.

In each case, growth is increased, cell cycle exit is delayed and cells are much more resistant to proapoptotic signals. Moreover, elevated levels of cyclin E and DIAP1 are observed in all three mutants. Our binding experiments show that Hpo requires its C terminus to bind to Sav. While this association appears to be mediated by the N-terminal portion of Sav, it is possible that the coiled-coil domain of Sav also participates in this interaction. Wts appears to bind to a different portion of Sav, the WW domains. Consistent with these observations, increased amounts of Wts do not reduce binding of Hpo to Sav. These studies favor a model where Sav acts as a scaffold that simultaneously binds both Hpo and Wts and that these three proteins function together to modulate cyclin E and DIAP1 levels. Consistent with this model, reducing Hpo levels decreases apoptosis induced by the combined overexpression of Sav and Wts. An alternate explanation is that Hpo and Wts bind separately to different pools of Sav and that Sav-Hpo and Sav-Wts complexes function additively in parallel pathways to promote apoptosis. A more precise definition of Hpo, Sav, and Wts complexes requires detailed biochemical analysis of endogenous protein complexes.

Regulation of Apoptosis by Hpo and Sav

hpo, *sav*, and *wts* are each required for the apoptosis of supernumerary interommatidial cells, indicating that all three genes function in executing developmentally regulated apoptosis. Moreover, apoptosis induced by proteins such as Rpr, Hid, or Grim appears to require the function of each of these genes. Since DIAP1 levels are elevated in mutant clones, *hpo*, *sav*, and *wts* may function together to promote apoptosis by downregulating DIAP1 levels. This regulation may occur, at least in part, by the regulation of DIAP1 protein degradation. We have not observed substantial changes in DIAP1 RNA levels in *hpo* mutant tissue either by in situ hybridization or by semiquantitative RT-PCR. In the absence of a definitive null allele of *hpo*, additional modes of regulation involving changes in transcription, RNA processing or translation cannot be excluded.

A complex associated with Hpo or Sav can phosphorylate DIAP1 in vitro. Since these complexes likely include both Hpo and Wts, we do not know which of these kinases acts as the "effector kinase" in DIAP1 phosphorylation. Moreover, since these experiments used reticulocyte lysates, the phosphorylation of DIAP1 could either be direct or may require other kinases present in the complex pulled down from the lysate. Nevertheless, they provide preliminary evidence that a Sav/Hpo complex can initiate a chain of events that culminates in DIAP1 phosphorylation. Whether Hpo, Sav, and Wts indeed promote phosphorylation-dependent instability of DIAP1 in vivo requires further investigation. Moreover, the possibility exists that Hpo also regulates apoptosis by phosphorylating proteins other than DIAP1.

Our experiments that assess the consequences of DIAP1 phosphorylation on the regulation of its stability made the assumption that either DIAP1 or a protein found in the reticulocyte lysate can function as an E3 enzyme that promotes DIAP1 degradation. It is conceivable that another protein might provide this function in vivo. However, even under the conditions of our experiment, where all of the DIAP1 is unlikely to be phosphorylated, we have observed a reproducible effect on DIAP1 stability. These findings are consistent with a model where two different proapoptotic pathways, one featuring Rpr, Hid, and Grim and the other involving Sav, Wts, and Hpo converge to regulate DIAP1 stability. Added to this is the recent observation that the degradation of DIAP1 also requires cleavage by caspases (Ditzel et al., 2003). Since caspases can be activated by a variety of upstream signals, DIAP1 may function as an integrator of multiple pathways that regulate apoptosis.

Concluding Remarks

sav has a single human ortholog, hWW45, and we have previously shown that this gene is deleted in two different cell lines derived from kidney cancers (Tapon et al., 2002). Inactivation of one of the two mammalian orthologs of *wts*, Lats1, resulted in slow-growing tumors in mice (St John et al., 1999). It therefore seems likely that Mst1 and Mst2, may function as tumor-suppressor genes in mammals.

Experimental Procedures

Fly Stocks

w; FRT42D males were mutagenized with ethylmethanesulfonate, then crossed to either *y w eyFLP; FRT42D P[mini-w, armLacZ]* or first to *w; CyO/Sco*, then individually to *y w eyFLP; FRT42D P[mini-w, armLacZ]*. Flies with eyes that contained more white than red tissue were retained and maintained as balanced stocks. Three alleles of *hpo* were identified; hpo^{MGH1}, hpo^{MGH2}, and hpo^{MGH3}. *GMR-grim* (on the third chromosome) was from John Abrams. *GMR-sav, GMR-wts* have been described (Tapon et al., 2002). Other stocks included *y w eyFLP; FRT42D P[mini-w, UbiGFP]*, *y w hsFLP; FRT42D P[ry+] hs-neo FRT42D P[ry+;w+]47A*, *y w hsFLP; FRT42D P[mini-w] P[UbiGFP]/SM6-TM6B* and *w; FRT40A* bsk^{170B} (Suzanne et al., 2001), *y w eyFLP; FRT40A P[mini-w, armLacZ]*, and *y w eyFLP glass-lacZ; FRT42D* w^{+} *cl2R11/CyO,* y^{+}.

Microscopy, Immunohistochemistry, and Flow Cytometry

For adult eye pictures, genotypes were as follows: *y w eyFLP/+; FRT42D/FRT42D P[mini-w] P[armLacZ]* and *y w eyFLP/+; FRT42D* hpo^{MGH1}*/FRT42D P[mini-w] P[armLacZ]*. For adult wing pictures and eye sections genotypes were as follows: *y w hsFLP/+; FRT42D/P[ry+] hs-neo FRT42D P[ry+;w+]47A* and *y w hsFLP/+; FRT42D* $hpo^{MGH1/3}$*/P[ry+] hs-neo FRT42D P[ry+;w+]47A]*. For eye SEMs, genotypes were: *w; Cyo/+ ; GMR-Grim/+, y w eyFLP/+; FRT42D* hpo^{MGH1}*/FRT42D P[mini-w] P[armLacZ] ; GMR-Grim/+,w Cyo/+; GMR-sav GMR-wts/+, y w eyFLP/+; FRT42D* hpo^{MGH1}*/FRT42D P[mini-w] P[armLacZ]; GMR-sav GMR-wts/+*.

Imaginal disc BrdU incorporations utilized a 1.5 hr BrdU pulse. Antibodies used were: antirabbit-Cy5 and antimouse Cy3 (Jackson Laboratories); anti-BrdU (Becton Dickinson); anti-phosH3 (Upstate Laboratories); anti β-galactosidase (Cappel); anti-cyclin E was from Helena Richardson (Richardson et al., 1995); anti DIAP1 was from Bruce Hay (Yoo et al., 2002); and anti-Discs-large was from the Developmental Studies Hybridoma Bank.

For FACS analysis, larval wing imaginal discs were heat shocked 48 hr AED, dissected 120 hr AED, dissociated in trypsin, and stained with Hoechst (Neufeld et al., 1998). Samples were run on a Cytomation MoFlo instrument with a 450/65nm filter and data were analyzed using FlowJo (Tree Star Inc.).

For doubling time experiments, *hpo* clones were induced 48 hr AED, and discs were dissected for analysis 120 hr AED. For FACS analysis and wing clone counts, genotypes were *y w hsFLP; FRT42D* hpo^{MGH1}*/FRT42D P[mini-w] P[UbiGFP]* and *y w hsFLP; FRT42D/FRT42D P[mini-w] P[UbiGFP]*.

For immunofluorescence, discs were dissected from the following genotypes: *y w eyFLP; FRT42D/FRT42D P[mini-w] P[UbiGFP]* and

y w eyFLP; FRT42D hpo$^{MGH1/3}$/FRT42D P[mini-w] P[UbiGFP]. For TUNEL stainings in a *GMR-grim* transgenic background, genotypes were: *y w eyFLP, FRT42D P[mini-w] P[armLacZ]/+; GMR-grim* and *y w eyFLP; FRT42D hpo^{MGH1}/FRT42D P[mini-w] P[armLacZ]; GMR-grim*. TUNEL positive nuclei were detected with a Rhodamine-conjugated anti-DIG antibody (Boehringer).

Characterization of the *hpo* Locus

hpo^{MGH1} and *hpo^{MGH3}* alleles complemented all stocks in the 2R deficiency kit. Mapping proceeded by meiotic recombination methods. 175 recombinant alleles were generated between the FRT42D *hpo^{MGH1}* chromosome and a distal P element-containing chromosome, EP0755, previously analyzed for SNPs by Berger et al. (2001). 125 recombinants complemented the *hpo^{MGH2}* allele, and 50 recombinants failed to complement the *hpo^{MGH2}* allele. Analysis of these recombinants at reported PLPs and SNPs along 2R mapped the mutation to a 165 kb region between 56D2 and 56D15-56E1. Sequencing of candidate genes in this area revealed nonsense mutations in the gene CG11228 in all three *hpo* alleles. Stocks used were *y w eyFLP; EP0755* and *y w eyFLP; FRT42D* (Berger et al., 2001).

Expression and Purification of Recombinant Proteins

GST-DIAP1 was produced from a GST-TEV-DIAP1-D20E plasmid provided by B. Hay (Yoo et al., 2002). The coding regions of the indicated genes or indicated subdomains were cloned into pMAL-TEV (MBP-tag), pET28 (His6), pCS2+ (IVT), and Myc-pCS2+ vectors (IVT). BL21 (DE3) competent cells were transformed with GST-TEV-DIAP1-D20e, pMAL-TEV, and pET28 constructs, grown in large-scale cultures, and induced with 1 mM IPTG for 4 hr. Hpo pET constructs were cotransformed with a thioredoxin plasmid. Bacterial lysates were incubated with glutathione Sepharose (GST-DIAP1), amylose resin (MBP-tagged proteins), or nickel beads (His-tagged proteins) in batch buffer and washed in buffer containing 300 mM NaCl. Proteins were used either coupled to beads or were eluted with maltose (MBP-tagged proteins) or imidazole (His-tagged proteins).

Tissue Culture, Transfections, and RNAi

Drosophila S2 cells were cultured in Schneider's medium containing 10% fetal calf serum at 25°C. Cells were transiently transfected using Cellfectin (GibcoBRL) and harvested 36 hr later. S2 cells were treated with RNAi by the soaking method and harvested at day 5.

In Vitro Binding Assays

Cold IVT Myc-tagged proteins were bound to anti-Myc coated protein A Sepharose beads. ^{35}S-labeled IVT candidate binding partners were added in the presence of 0.1 μg/ml cyclohexamide in binding buffer (50 mM HEPES [pH 7.7], 300 mM NaCl, 1 mM EDTA, and 0.1% Tween 20) and incubated at 4°C for 2 hr with gentle rocking. Binding reactions were washed, eluted, and subjected to SDS-PAGE. Bacterially expressed MBP-tagged proteins were bound to amylose resin, incubated with ^{35}S-labeled IVT candidate binding proteins, washed, eluted, and subjected to SDS-PAGE under the same conditions as the Myc-tagged binding assays.

In Vitro Kinase and Degradation Assays

MBP or MBP-Sav coupled to amylose resin were incubated in control IVT reactions (no template DNA added) or to IVT reactions containing wild-type Hpo and washed as in the binding assays. Beads were then washed in kinase buffer (25 mM Tris [pH 7.9], 10 mM β-glycerophosphate, 10 mM NaF, 10 mM $MgCl_2$, and 1 mM EDTA). Substrate was added in the presence of 10 μCi [γ-^{32}P]ATP and incubated for 30 minutes at room temperature. Reactions were quenched with sample buffer and subjected to SDS-PAGE. Alternatively, protein A Sepharose beads and anti-Myc antibody were incubated in IVT reactions containing MT alone or MT-Hpo and washed. Purified IVT MT or IVT MT-Hpo was incubated with substrate in kinase buffer and 10 μCi [γ-^{32}P]ATP as above. Degradation assays of IVT DIAP1 were incubated in either a cold IVT reaction control or cold IVT Hpo each supplemented with 100 ng bacterially expressed His-tagged E1, 100 ng bacterially expressed His-tagged Effete (E2), 1 mg/ml ubiquitin (Sigma), 0.1 mg/ml cyclohexamide, and an energy-regenerating system (7.5 mM creatine phosphate, 1 mM ATP, and 1 mM MgCl2). Initial and final time points were quenched in sample buffer and subjected to SDS-PAGE. Mass spectrometry of phosphorylated GST-DIAP1 was performed by the Taplin Biological Mass Spectrometry Facility.

Acknowledgments

We thank W. Fowle for generating the SEMs; B. Hay, J. Abrams, H. Richardson, K. White, the Bloomington Stock Center, and the Developmental Studies Hybridoma Bank for fly stocks, antibodies, and reagents; J. Jetz-Arruda for help with FACS analysis; P. Lueras for technical assistance; J. Avruch, K. Moberg, and R. Sordella for valuable advice; L. Madden for help with DNA sequencing; R. Tomaino for mass spectrometry; N. Tapon for providing fly stocks and for communication of unpublished results; and K. White for comments on the manuscript. K.F.H is the recipient of a HFSP long-term fellowship, C.M.P. is a fellow of the Jane Coffin Childs Memorial Fund for Medical Research, and I.K.H. was funded in part by the NIH (GM61672 and CA95281) and is a Faculty Scholar of the Richard Saltonstall Foundation.

Received: May 28, 2003
Revised: July 9, 2003
Accepted: July 9, 2003
Published online: July 15, 2003

References

Berger, J., Suzuki, T., Senti, K.A., Stubbs, J., Schaffner, G., and Dickson, B.J. (2001). Genetic mapping with SNP markers in Drosophila. Nat. Genet. *29*, 475–481.

Chang, L., and Karin, M. (2001). Mammalian MAP kinase signalling cascades. Nature *410*, 37–40.

Chen, P., Nordstrom, W., Gish, B., and Abrams, J.M. (1996). grim, a novel cell death gene in Drosophila. Genes Dev. *10*, 1773–1782.

Cheung, W.L., Ajiro, K., Samejima, K., Kloc, M., Cheung, P., Mizzen, C.A., Beeser, A., Etkin, L.D., Chernoff, J., Earnshaw, W.C., and Allis, C.D. (2003). Apoptotic phosphorylation of histone H2B is mediated by mammalian sterile twenty kinase. Cell *113*, 507–517.

Creasy, C.L., and Chernoff, J. (1995a). Cloning and characterization of a human protein kinase with homology to Ste20. J. Biol. Chem. *270*, 21695–21700.

Creasy, C.L., and Chernoff, J. (1995b). Cloning and characterization of a member of the MST subfamily of Ste20-like kinases. Gene *167*, 303–306.

Dan, I., Watanabe, N.M., and Kusumi, A. (2001). The Ste20 group kinases as regulators of MAP kinase cascades. Trends Cell Biol. *11*, 220–230.

Ditzel, M., Wilson, R., Tenev, T., Zachariou, A., Paul, A., Deas, E., and Meier, P. (2003). Degradation of DIAP1 by the N-end rule pathway is essential for regulating apoptosis. Nat. Cell Biol. *5*, 467–473.

Goyal, L., McCall, K., Agapite, J., Hartwieg, E., and Steller, H. (2000). Induction of apoptosis by Drosophila reaper, hid and grim through inhibition of IAP function. EMBO J. *19*, 589–597.

Graves, J.D., Gotoh, Y., Draves, K.E., Ambrose, D., Han, D.K., Wright, M., Chernoff, J., Clark, E.A., and Krebs, E.G. (1998). Caspase-mediated activation and induction of apoptosis by the mammalian Ste20-like kinase Mst1. EMBO J. *17*, 2224–2234.

Grether, M.E., Abrams, J.M., Agapite, J., White, K., and Steller, H. (1995). The head involution defective gene of Drosophila melanogaster functions in programmed cell death. Genes Dev. *9*, 1694–1708.

Hays, R., Wickline, L., and Cagan, R. (2002). Morgue mediates apoptosis in the Drosophila melanogaster retina by promoting degradation of DIAP1. Nat. Cell Biol. *4*, 425–431.

Holley, C.L., Olson, M.R., Colon-Ramos, D.A., and Kornbluth, S. (2002). Reaper eliminates IAP proteins through stimulated IAP degradation and generalized translational inhibition. Nat. Cell Biol. *4*, 439–444.

Igaki, T., Kanda, H., Yamamoto-Goto, Y., Kanuka, H., Kuranaga, E.,

Aigaki, T., and Miura, M. (2002). Eiger, a TNF superfamily ligand that triggers the Drosophila JNK pathway. EMBO J. *21*, 3009–3018.

Justice, R.W., Zilian, O., Woods, D.F., Noll, M., and Bryant, P.J. (1995). The Drosophila tumor suppressor gene warts encodes a homolog of human myotonic dystrophy kinase and is required for the control of cell shape and proliferation. Genes Dev. *9*, 534–546.

Kango-Singh, M., Nolo, R., Tao, C., Verstreken, P., Hiesinger, P.R., Bellen, H.J., and Halder, G. (2002). Shar-pei mediates cell proliferation arrest during imaginal disc growth in Drosophila. Development *129*, 5719–5730.

Khokhlatchev, A., Rabizadeh, S., Xavier, R., Nedwidek, M., Chen, T., Zhang, X.F., Seed, B., and Avruch, J. (2002). Identification of a novel Ras-regulated proapoptotic pathway. Curr. Biol. *12*, 253–265.

Lee, K.K., Murakawa, M., Nishida, E., Tsubuki, S., Kawashima, S., Sakamaki, K., and Yonehara, S. (1998). Proteolytic activation of MST/Krs, STE20-related protein kinase, by caspase during apoptosis. Oncogene *16*, 3029–3037.

Lisi, S., Mazzon, I., and White, K. (2000). Diverse domains of THREAD/DIAP1 are required to inhibit apoptosis induced by REAPER and HID in Drosophila. Genetics *154*, 669–678.

Marygold, S.J., and Leevers, S.J. (2002). Growth signaling: TSC takes its place. Curr. Biol. *12*, R785–787.

Moreno, E., Yan, M., and Basler, K. (2002). Evolution of TNF signaling mechanisms: JNK-dependent apoptosis triggered by Eiger, the Drosophila homolog of the TNF superfamily. Curr. Biol. *12*, 1263–1268.

Neufeld, T.P., de la Cruz, A.F., Johnston, L.A., and Edgar, B.A. (1998). Coordination of growth and cell division in the Drosophila wing. Cell *93*, 1183–1193.

Oldham, S., and Hafen, E. (2003). Insulin/IGF and target of rapamycin signaling: a TOR de force in growth control. Trends Cell Biol. *13*, 79–85.

Prober, D.A., and Edgar, B.A. (2000). Ras1 promotes cellular growth in the Drosophila wing. Cell *100*, 435–446.

Richardson, H., and Kumar, S. (2002). Death to flies: Drosophila as a model system to study programmed cell death. J. Immunol. Methods *265*, 21–38.

Richardson, H., O'Keefe, L.V., Marty, T., and Saint, R. (1995). Ectopic cyclin E expression induces premature entry into S phase and disrupts pattern formation in the Drosophila eye imaginal disc. Development *121*, 3371–3379.

Riesgo-Escovar, J.R., Jenni, M., Fritz, A., and Hafen, E. (1996). The Drosophila Jun-N-terminal kinase is required for cell morphogenesis but not for DJun-dependent cell fate specification in the eye. Genes Dev. *10*, 2759–2768.

Ryoo, H.D., Bergmann, A., Gonen, H., Ciechanover, A., and Steller, H. (2002). Regulation of Drosophila IAP1 degradation and apoptosis by reaper and ubcD1. Nat. Cell Biol. *4*, 432–438.

Sluss, H.K., Han, Z., Barrett, T., Davis, R.J., and Ip, Y.T. (1996). A JNK signal transduction pathway that mediates morphogenesis and an immune response in Drosophila. Genes Dev. *10*, 2745–2758.

St John, M.A., Tao, W., Fei, X., Fukumoto, R., Carcangiu, M.L., Brownstein, D.G., Parlow, A.F., McGrath, J., and Xu, T. (1999). Mice deficient of Lats1 develop soft-tissue sarcomas, ovarian tumours and pituitary dysfunction. Nat. Genet. *21*, 182–186.

Suzanne, M., Perrimon, N., and Noselli, S. (2001). The Drosophila JNK pathway controls the morphogenesis of the egg dorsal appendages and micropyle. Dev. Biol. *237*, 282–294.

Tapon, N., Harvey, K.F., Bell, D.W., Wahrer, D.C., Schiripo, T.A., Haber, D.A., and Hariharan, I.K. (2002). salvador promotes both cell cycle exit and apoptosis in Drosophila and is mutated in human cancer cell lines. Cell *110*, 467–478.

Taylor, L.K., Wang, H.C., and Erikson, R.L. (1996). Newly identified stress-responsive protein kinases, Krs-1 and Krs-2. Proc. Natl. Acad. Sci. USA *93*, 10099–10104.

Wang, S.L., Hawkins, C.J., Yoo, S.J., Muller, H.A., and Hay, B.A. (1999). The Drosophila caspase inhibitor DIAP1 is essential for cell survival and is negatively regulated by HID. Cell *98*, 453–463.

White, K., Grether, M.E., Abrams, J.M., Young, L., Farrell, K., and Steller, H. (1994). Genetic control of programmed cell death in Drosophila. Science *264*, 668–669.

Wilson, R., Goyal, L., Ditzel, M., Zachariou, A., Baker, D.A., Agapite, J., Steller, H., and Meier, P. (2002). The DIAP1 RING finger mediates ubiquitination of Dronc and is indispensable for regulating apoptosis. Nat. Cell Biol. *4*, 445–450.

Wing, J.P., Schreader, B.A., Yokokura, T., Wang, Y., Andrews, P.S., Huseinovic, N., Dong, C.K., Ogdahl, J.L., Schwartz, L.M., White, K., and Nambu, J.R. (2002). Drosophila morgue is an F box/ubiquitin conjugase domain protein important for grim-reaper mediated apoptosis. Nat. Cell Biol. *4*, 451–456.

Xu, T., Wang, W., Zhang, S., Stewart, R.A., and Yu, W. (1995). Identifying tumor suppressors in genetic mosaics: the Drosophila lats gene encodes a putative protein kinase. Development *121*, 1053–1063.

Yang, Y., Fang, S., Jensen, J.P., Weissman, A.M., and Ashwell, J.D. (2000). Ubiquitin protein ligase activity of IAPs and their degradation in proteasomes in response to apoptotic stimuli. Science *288*, 874–877.

Yoo, S.J., Huh, J.R., Muro, I., Yu, H., Wang, L., Wang, S.L., Feldman, R.M., Clem, R.J., Muller, H.A., and Hay, B.A. (2002). Hid, Rpr and Grim negatively regulate DIAP1 levels through distinct mechanisms. Nat. Cell Biol. *4*, 416–424.

Note Added in Proof

In the accompanying paper, Wu et al. present an independent characterization of the *hippo* gene. Using a null allele of *hippo*, they demonstrate increased DIAP1 transcription in mutant cells. The alleles used in our study are likely to be hypomorphs. Our analysis of these alleles provides evidence for posttranscriptional regulation of DIAP1 by Hippo.